Electronic Letters on Computer Vision and Image Analysis 21(1):28-46, 2022

Retinal Blood Vessels Segmentation using Fréchet PDF and MSMO Method

Sushil Kumar Saroj*, Rakesh Kumar* and Nagendra Pratap Singh+

* *Department of computer science and engineering, MMMUT, Gorakhpur, India*
+ *Department of computer science and engineering, NIT, Hamirpur, India*

Received 18th of June, 2021; accepted 5th of March, 2022

Abstract

Abstract: Blood vessels of retina contain information about many severe diseases like glaucoma, hypertension, obesity, diabetes etc. Health professionals use this information to detect and diagnose these diseases. Therefore, it is necessary to segment retinal blood vessels. Quality of retinal image directly affects the accuracy of segmentation. Therefore, quality of image must be as good as possible. Many researchers have proposed various methods to segment retinal blood vessels. Most of the researchers have focused only on segmentation process and paid less attention on pre processing of image even though pre processing plays vital role in segmentation. The proposed method introduces a novel method called multi-scale switching morphological (MSMO) for pre processing and Fréchet match filter for retinal vessel segmentation. We have experimentally tested and verified the proposed method on DRIVE, STARE and HRF data sets. Obtained outcome demonstrate that performance of the proposed method has improved substantially. The cause of improved performance is the better pre processing and segmentation methods.

Key Words: Image enhancement, MSMO Operator, Segmentation, Fréchet PDF.

1 Introduction

Illness in any form is not desirable and everyone wants to get rid of it. There are numbers of severe diseases which affect human life badly today. Some of them are hypertension, diabetes, glaucoma, obesity, macular degeneration, arthritis etc. Glaucoma and diabetes can cause vision loss too. Diabetic, obesity and hypertension are the bases for several deadliest diseases. Diseases are generally identified either by their symptoms or by color and structure. Diabetes, glaucoma, obesity, macular degeneration, hypertension etc. can be identified by observing color and structure of retinal vessels. Hence, segmentation of retinal's vessels is necessary. During the process of capturing and transmission of retinal images, several factors affect the quality of the images. Generally, retinal images are too dark, too bright, unclear and have poor contrast, noises, artificial colors, etc. Due to these, quality of retinal images is generally poor. Quality of a retinal image directly affects the accuracy of segmentation of vessels. Therefore, there is need an approach for better image enhancement as well as segmentation of retinal vessels [17][18].

Correspondence to: sushil.mnnit10@gmail.com
Recommended for acceptance by Angel D. Sappa
https://doi.org/10.5565/rev/elcvia.1453
ELCVIA ISSN: 1577-5097
Published by Computer Vision Center / Universitat Autonoma de Barcelona, Barcelona, Spain

Image enhancement has always been challenging and main task of image processing. Characteristics of retinal images make it more tedious. In the mean, there is need an appropriate method for retinal image enhancement. There are existing various methods today for image enhancement. These are classified as in the Figure 1. Various approaches are given by many researchers for image enhancement, but they are not efficient and have scope of improvement.

In the proposed approach, we have applied the MSMO operator along with principal-component analysis (PCA) and contrast-limited adaptive histogram equalization (CLAHE) methods for pre processing and Fréchet match-filter for vessel segmentation. MSMO operator is a morphological operator. It is used to enhance the retinal images. It is more efficient and gives better results for not only retinal images but also for MRI, ultrasound, X-ray images etc. too. Fréchet match filter is a latest and one of the best segmentation methods for retinal vessels. Fréchet match filter performs better than others when it is applied on enhanced grayscale image by the MSMO operator. The main objective of this literature is to maximize the accuracy of segmentation. The proposed method is more efficient as well as robust. The major contributions of the literature are:

- Detailed study of various image enhancement techniques.
- Design of a methodology based on MSMO operator for retinal or medical image enhancement.
- Design of a novel approach based on MSMO operator and Fréchet PDF for better segmentation.
- Conducted in-depth experiments on large numbers of images to examine and verify the method.

Remaining part of the literature is arranged as: In Section-2, various related findings are investigated for better image enhancement and vessel's segmentation. In Section-3, a novel approach is presented for better image enhancement and vessel's segmentation. In Section-4, performance of the method is analyzed. At last, the method is concluded in Section-5.

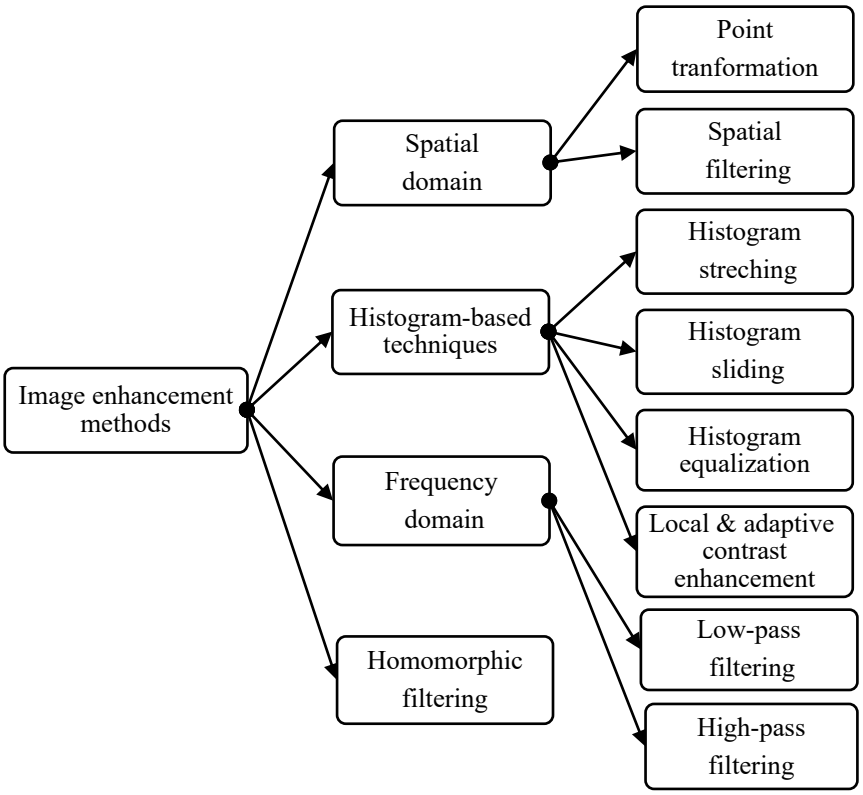

Figure 1: Taxonomy of image enhancement techniques

2 Related Work

The Sobel, Canny, Gradient, and Prewitt operators are the classical methods for edge detection. They work well when edges are distinct as well as sharp. Although, retinal blood vessels are generally thin and entangled. Intensities of vessels change gradually and contrast between vessels and their background are generally very low. In these scenarios, these classical methods fail to detect retinal vessels [23][24][25][29].

Accuracy of vessels segmentation produced by various methods is generally low. The main reason behind this is retinal vessel has very low contrast corresponding to its background. Contrast between vessel and its background can be increased by applying an efficient image enhancement method. Therefore, there is required an approach that not only good in vessel segmentation but also in pre processing. In search of this, various prominent methods based on pre processing and segmentation of retinal vessels are investigated. Some of them are discussed below [2][10]:

Singh et al. [7] have given an approach for vessels segmentation. In the approach, they have used the PCA and CLAHE methods to improve the quality of retinal images. They have applied the Gumbel match filter on obtained enhanced retinal images to generate the match-filter response (MFR) images. Author has applied the optimal thresholding technique to extract the retinal vessels from MFR images. They said that vessel profile shape does not oriented uniformly towards its trunk-value but little bit skewed. In contrast, Gumbel PDF is also little bit skewed about its trunk-point. Hence, author has implemented the Gumbel PDF as the kernel for their match filter. Even though, vessel- profile shape is not really Gumbel-curve shape. It is Fréchet curve shape. Image enhanced by above methods is not so good. Also, accuracy of segmentation is low.

Kaba et al. [8] have introduced a method for retinal vessels segmentation. In their approach, they have used the adaptive histogram equalization and bias correction in pre processing stage to enhance the retinal images. They have applied the probabilistic modelling on obtained enhanced images to extract the vessels. Expectation maximization technique is used for optimization. This model is effective only in tracking-based scenario. The model reduces width of original vessel. Enhanced images using the adaptive histogram equalization and bias correction is not good enough. Due to which accuracy of segmentation is poor.

Odstrcilk et al. [4] have designed a method for vessel's segmentation. In the approach, they have used contrast equalization and illumination correction techniques in the pre processing stage for image enhancement. They have used green channel of RGB image. Based on widths of vessels, intensity profiles of vessels are divided into five categories here. The author has designed five two-dimensional match filter kernels for each image. Due to five match filter kernels for each image, computational complexity increased five times. Also, accuracy of the model relies on how accurately the author divides intensity profile into five parts.

Zhou et al. [5] have given an approach for vessels segmentation. In the approach, author has applied the 2 D Gabor wavelet for image smoothing and a mathematical operation for contrast normalization and luminosity equalization in the pre processing stage. They have applied convolutional neural network (CNN) and dense CRF method for segmentation of vessels. Image enhanced by above methods is good but not sufficient due to which accuracy is comparatively low.

GeethaRamani et al. [21] have proposed an algorithm for vessels segmentation. In their literature, they have used the Gabor filter and Halfwave rectification methods in pre processing stage to crop image, transform color and extraction color channel. From preprocessing stage, we obtain a feature vector. The PCA method is applied on this feature vector. Thereafter, k means clustering technique is applied on obtained result to categories pixels in the vessels and non-vessels groups. Ensemble classifier removes the non vessel group. The model is quite complex. Image enhanced in preprocessing stage is not good enough due to which accuracy of segmentation is low.

Memari et al. [1] have introduced a method for vessel-segmentation. In this literature, the author has applied the CLAHE and mathematical morphology methods for retinal image enhancement. The author has used the Frangi and Gabor match filters to enhance the vessels networks. The Improved spatial fuzzy c means using genetic algorithm is applied for vessels segmentation. The model has high computational overhead. Retinal images enhanced by this method is not so good. Also, accuracy of segmentation of the model is relatively low.

Saroj et al. [6] have proposed a method for vessel's segmentation. In their literature, they have applied the PCA and CLAHE methods for retinal image enhancement. They have applied the Fréchet match filter for segmentation of vessels. They have tested their approach on STARE as well as DRIVE data sets. Although, segmentation method is efficient and good but methods used for image enhancement seems inappropriate and less efficient. Due to which, method did not perform as it could.

The methodology proposed in the literature involves a novel method for image enhancement and an efficient match filter for vessels segmentation. Blood vessels of retina have usually very low contrast with their background due to which vessels are not fully extracted from their backgrounds. MSMO is a novel and efficient method which enhances contrast between vessels and their backgrounds. Match filter method increases the contrast of retinal image. Hence, match-filter method identifies retinal blood vessels more correctly than other segmentation methods. Since Fréchet match filter is a latest and efficient match filter, we use this for vessel segmentation in the literature. Fréchet match filter along with MSMO method produced higher accuracy.

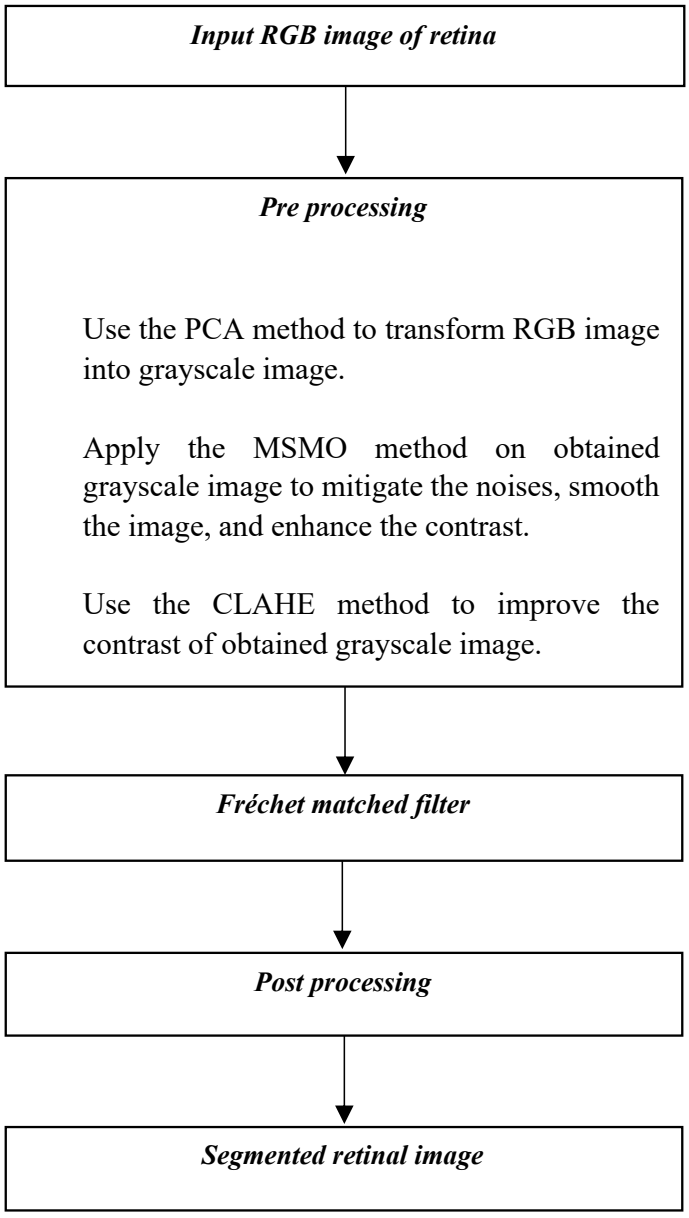

Figure 2: Block diagram of the proposed method

3 Proposed Method

The proposed method is based on a novel image enhancement technique i.e. the MSMO method and a best-known match filter i.e. Fréchet match filter for vessel segmentation. There are involved numbers of image operations in the approach which are grouped in the three major phases viz; pre processing, Fréchet match filter and post processing. Figure 2 shows these image-processing phases.

3.1 Pre-processing

Retinal vessels have few specific properties. Retinal vessels become thinner as we proceed out from optic disk. Intensity of retinal vessels change smoothly. Also, contrast between retinal vessel and its background is usually very low. Due to these characteristics, it is very hard to detect retinal blood vessels. Hence, to increase accuracy of vessel's segmentation, there is required to enhance the quality of retinal images. To achieve this, pre-processing of retinal image is needed. Generally, researchers emphasize more on only segmentation methods and pay less attention on pre processing although pre processing plays vital role in vessels segmentation. Therefore, we introduced a novel and efficient method i.e. the MSMO method for image enhancement. In the literature, pre processing module has three steps which are described as follows:

3.1.1 PCA Method

As we know that almost all the methods work on grayscale images. Therefore, it become necessary to convert RGB image into grayscale image. Most of the authors have used the rgb2gray method of MATLAB for this purpose. One more method called PCA is also exploited for this purpose. PCA method [12] has several advantages over rgb2gray method such as it preserves texture as well as color properties discriminability effectively. Also, it does not require any user specific parameter for conversion. Therefore, we use PCA for RGB to grayscale image conversion in the literature. But alone PCA method does not do much for image enhancement.

3.1.2 MSMO Method

We know that morphological operations such as dilation or erosion works on two inputs i.e. the grayscale image and structure element. Dilation $(\oplus)$ as well as erosion $(\ominus)$ operations on gray-scale image 'A' using structure element 'B' are defined by equation (1) and (2).

$$D = A \oplus B = \{(x, y) + (u, v) : x, y \in A; u, v \in B\}; \tag{1}$$

$$E = A \ominus B = \{(x, y) - (u, v) : x, y \in A; u, v \in B\}; \tag{2}$$

SMO is a morphological operator that uses the dilation and erosion operations as its sub functions. The operation dilation or erosion increases or decreases the tiny regions of an image according to size of structure element. Then matching with actual image, outcome of erosion or dilation operation primarily modifies tiny regions of the image. Due to this, SMO smooths regions of the image and replaces grey values of tiny regions with grey values of dilation or erosion operation. SMO is defined as follows:

if $((D - A) < (A - E))$ **then**
    SMO=D;
else
    if $((D - A) > (A - E))$ **then**
        SMO=E;
    else
        SMO=A;

end if
end if

Above definition of SMO implies that every pixel of enhanced image by SMO is particularly substituted by the same pixel in dilation, erosion results with a grey-value which is closed to grey-value of same pixel in the actual image. However, SMO with small size structure element is less efficient whereas SMO with large size structure element yields more noise. To reduce noise and make SMO more efficient, it is applied at multiple stages with structure elements having different sizes. Since SMO is applied on multiple scales with varying size of structure elements, it is called multi-scale SMO (MSMO). Some most frequently applied shapes into the structure elements are circle, square, hexagon and rectangle. Hexagon, rectangle and square shapes of structure elements generally have rough edges and yield block-effect which crash image region shape, particularly when structure element size is large. Circle shape of structure element has smooth edge due to which block-effect is very low. Hence, we opt circle shape as a shape of structure element in our literature. Scale number (n) is essential factor in the MSMO. Large n generally leads to heavy noise whereas small n is inefficient for retinal or medical image enhancement. The MSMO algorithm is described as follows:

Algorithm:

- Input gray scale image 'A' and structure element 'B'.
- Perform dilation as well as erosion operations on 'A' using 'B' with size s for every scale s $(1 \leq s \leq n)$.
- Outcome of SMO is computed for every scale s $(1 \leq s \leq n)$.
- End result is formed along pixel wise taking the mean of all multi-scale outputs generated by SMO.
- Get enhanced gray-scale image.

MSMO method is operated on gray scale image generated by PCA method. It removes noises. It smooths images. It also enhances the contrast. Due to these improvements, accuracy of vessel segmentation has increased substantially.

3.1.3 CLAHE Method

CLAHE method is designed to improve the contrast of an image. It can work with homogeneous as well as heterogeneous images. It can work with gray scale as well as color images too. Gray-scale image generated by CLAHE method has less noise. Although, there are a lot of advantages of the CLAHE method but alone CLAHE or together with PCA is not sufficient in many cases. In the literature, CLAHE is applied on the output of MSMO method. PCA, MSMO and CLAHE methods combination produce better quality of image [22].

Signal to noise ratio (SNR): It is a metric which is used to compare the quality of images.

$$SNR = \mu/\delta \tag{3}$$

where, μ is the mean of an image, and δ is the standard deviation of an image.

Figure 3 shows the grayscale images generated or enhanced by different pre processing methods. From the Figure 3, it is clear that image enhanced by PCA+MSMO+CLAHE method is better than the images enhanced by rgb2gray, PCA and PCA+CLAHE. If we observe the Tables 1-5 then we find that SNR values obtained by PCA+MSMO+CLAHE for all the images of all data sets mentioned above are greater than SNR values obtained by rgb2gray, PCA and PCA+CLAHE. Value of SNR of the image is determined by equation (3). Table 6 shows the accuracy of segmentation for all images of DRIVE data set. These accuracies are produced by the Fréchet match filter when it is operated on the enhanced grayscale images by different pre processing methods. From the Table 6, it is clear that accuracy of segmentation of enhanced gray scale image by the PCA+MSMO+CLAHE is higher than rgb2gray, PCA and PCA+CLAHE. Alone PCA and CLAHE or PCA+CLAHE is not sufficient for retinal image enhancement. When we use the MSMO method with PCA and CLAHE then this combination yields better results as we can see in Tables 1-6 and Figure 3. Due to these reasons, we have applied a

novel method called the MSMO method with PCA and CLAHE in PCA+MSMO+CLAHE sequence for image enhancement. The MSMO along with PCA and CLAHE methods not only produce better results for retinal images but also for other medical images such as MRI, Ultrasound X-ray etc. as we can see the results in the Tables 1-5. Figure 4 shows the segmented images generated by proposed method using different pre-processing methods where PCA+MSMO+CLAHE has segmented image better. In the Tables 1-6, R, P, M, and C stand for rgb2gray, PCA, MSMO, and CLAHE, respectively.

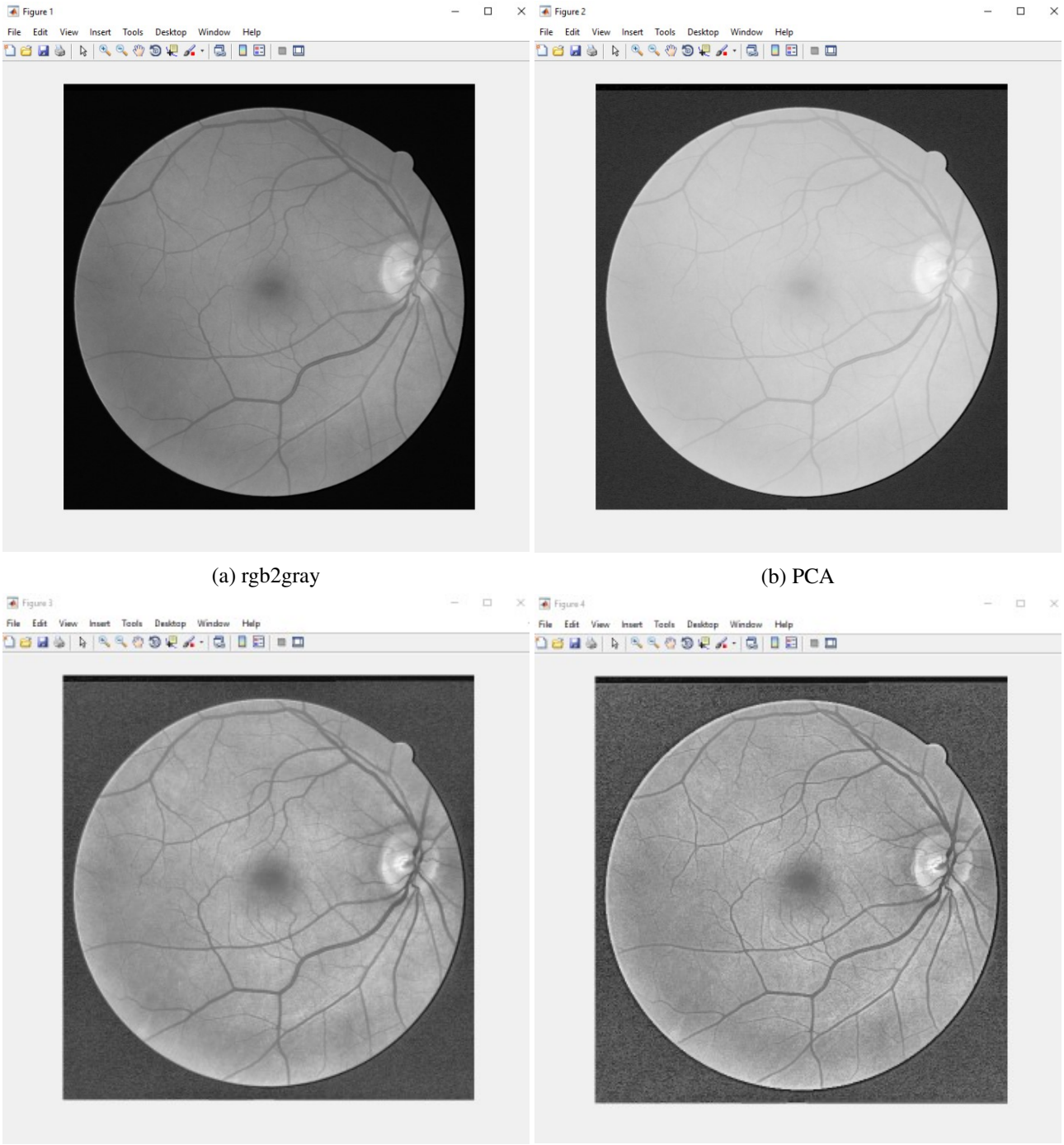

(a) rgb2gray (b) PCA

(c) PCA+CLAHE (d) PCA+MSMO+CLAHE

Figure 3: Enhanced retina images of 16_test.tif using different preprocessing methods

Img	R	P	P+C	P+M+C
1	1.5654	2.1813	3.1036	3.2095
2	1.5492	2.1407	3.0182	3.158
3	1.6276	2.3632	3.074	3.2388
4	1.4961	2.1583	3.0286	3.1563
5	1.5778	2.219	3.1367	3.2668
6	1.575	2.1844	3.0115	3.1019
7	1.5115	2.1581	2.9985	3.1212
8	1.5394	2.1793	3.0693	3.2084
9	1.5561	2.1441	3.087	3.2088
10	1.5563	2.2397	3.1987	3.2591
11	1.5127	2.1405	3.0198	3.1569
12	1.5665	2.1806	3.1186	3.1883
13	1.5409	2.1424	3.0469	3.1804
14	1.5757	2.2267	3.1678	3.2818
15	1.4596	2.2231	3.1943	3.2741
16	1.561	2.1467	3.0021	3.3339
17	1.5635	2.1298	2.9637	3.091
18	1.5528	2.134	3.0329	3.1721
19	1.581	2.263	3.0688	3.1272
20	1.5713	2.1945	3.1684	3.3093
Avg. SNR	1.55197	2.18747	3.07547	3.20219

Table 1: SNR values for DRIVE images generated by different pre processing methods

Img	P	P+C	P+M+C
1	3.4277	4.4735	4.4726
2	3.2003	4.3774	4.437
3	3.3071	4.346	4.371
4	3.1377	3.6631	3.7228
5	2.8765	3.7038	3.7305
6	3.5104	3.5949	3.9923
7	2.7693	3.6806	3.7418
8	3.2637	3.8562	3.8778
9	2.7061	3.6717	3.7503
10	3.6519	4.4218	4.4433
11	2.775	3.8532	3.9071
12	2.5788	3.7084	4.3809
13	2.5115	3.6173	4.4123
14	2.5849	3.6757	3.744
15	2.8587	3.7795	3.8341
16	3.3078	3.7437	3.7525
17	3.2437	4.1746	4.1935
18	3.1636	3.9573	3.9857
19	2.7536	3.666	3.7333
20	2.7691	3.547	3.615
Avg. SNR	3.01987	3.875585	4.00489

Table 2: SNR values for STARE images generated by different pre processing methods

Img	P	P+C	P+M+C
1	1.4243	2.3542	2.59
2	1.4673	2.3579	2.5489
3	1.3666	2.3553	2.5846
4	1.3956	2.3363	2.5834
5	1.3282	2.3328	2.6
6	1.3932	2.3581	2.6055
7	1.3432	2.3887	2.6678
8	1.316	2.3894	2.7419
9	1.43	2.3883	2.6662
10	1.4473	2.4028	2.6893
Avg. SNR	1.39117	2.36638	2.62776

Table 3: SNR values for MRI images generated by different pre processing methods

Img	P	P+C	P+M+C
1	1.8746	2.0749	2.121
2	1.5931	2.0108	2.0686
3	1.9389	2.1721	2.1605
4	1.8782	2.1426	2.1447
5	1.6902	2.0296	2.145
6	1.4474	1.9273	2.0343
7	1.1788	1.6269	1.7217
8	1.3016	1.7436	1.9029
Avg. SNR	1.61285	1.965975	2.0373375

Table 4: SNR values for Ultrasound images generated by different pre processing methods

Img	P	P+C	P+M+C
01_h	2.3549	2.8769	2.9667
02_h	2.3677	2.8603	2.9409
03 _h	2.3337	2.8775	2.9791
04_h	2.3054	2.7649	2.8093
05_h	2.3466	2.7794	2.8441
01_dr	2.3771	2.8213	2.9021
02_dr	2.3708	2.7507	2.8099
03_dr	2.3678	2.7402	2.8108
04_dr	2.3543	2.7548	2.8247
05_dr	2.3409	2.8162	2.8761
01_g	2.4062	2.972	3.332
02_g	2.3766	2.7994	2.8945
03_g	2.3758	2.8716	2.9466
04_g	2.3742	2.8665	2.9363
05_g	2.3612	2.8441	2.9257
Avg. SNR	2.36088	2.8263867	2.91992

Table 5: SNR values for HRF images generated by different pre processing methods

Img	R	P	P+C	P+M+C
1	0.8905	0.9108	0.9563	0.9581
2	0.9159	0.8976	0.9553	0.955
3	0.8929	0.9003	0.9397	0.9408
4	0.8947	0.908	0.9586	0.9572
5	0.9296	0.9063	0.9578	0.9583
6	0.9165	0.9027	0.9506	0.951
7	0.8709	0.9086	0.9521	0.9529
8	0.9127	0.914	0.9476	0.9494
9	0.9158	0.919	0.957	0.9537
10	0.9219	0.9177	0.9571	0.9593
11	0.8752	0.9105	0.952	0.955
12	0.8772	0.9137	0.9535	0.9534
13	0.8917	0.9022	0.9504	0.9481
14	0.864	0.9192	0.9569	0.9581
15	0.8685	0.9362	0.9519	0.9577
16	0.8918	0.9097	0.9576	0.9574
17	0.8763	0.9156	0.9551	0.9535
18	0.8925	0.9208	0.9631	0.9643
19	0.9141	0.917	0.9598	0.9669
20	0.9262	0.9265	0.9658	0.9653
Avg. Acc.	0.8969	0.9128	0.9549	0.9558

Table 6: Accuracy of the proposed method for DRIVE images using different pre processing methods

3.2 Fréchet PDF based Matched Filter

Fréchet PDF is also known as extreme value PDF. It has skewed properties. It is described as follows:

$$f(x,y) = \alpha/\beta((d-\gamma)/\beta) \wedge (-(1+\alpha))e \wedge (-((d-\gamma)/\beta) \wedge (-\alpha))\forall |y| \leq L/2 \tag{4}$$

where $\alpha > 0$, $\beta > 0$, f (x, y): Fréchet-kernel, (x, y): element's coordinate in the kernel, d: smallest distance between center and coordinate (x, y), L: vessel's segment, α: shape parameter, β: scale parameter, γ: location parameter. Initially, vessels are assumed to be oriented across y axis and Fréchet kernel at origin. In Fréchet match-filter, shape parameter (α) manages the shapes of Fréchet curve. We can match Fréchet kernel as near as shape of vessel-profile by choosing suitable value of α. Accuracy of a match filter method depends on how closely that match filter kernel matches with shape of vessel profile. Other match filter methods such as Cauchy, Gumbel and Gaussian etc. have no such parameter. Therefore, Fréchet match filter generates better accuracy than other match filter methods by choosing suitable value of α.

In the literature, large scale experiments are carried out on various retinal data sets to select appropriate values of α, β, γ, L and n for the Fréchet filter and MSMO operator. The method is practically tested for distinct values of α (varying from 1 to 5 having interval 1), β(varying from 0 to 5.0 having interval 0.5), γ(varying from 0 to 5.0 having interval 0.5), L (varying from 1 to 15 having interval 1) and n (varying from 1 to 15 having interval 1) for every image of DRIVE data set. We found average accuracy 95.74 % for α=1, β=1, γ=1.72, L=11 and n=5. The method is practically tested for distinct values of α (varying from 1 to 5 having interval 1), β(varying from 0 to 5.0 having interval 0.5), γ(varying from 0 to 5.0 having interval 0.5), L (varying

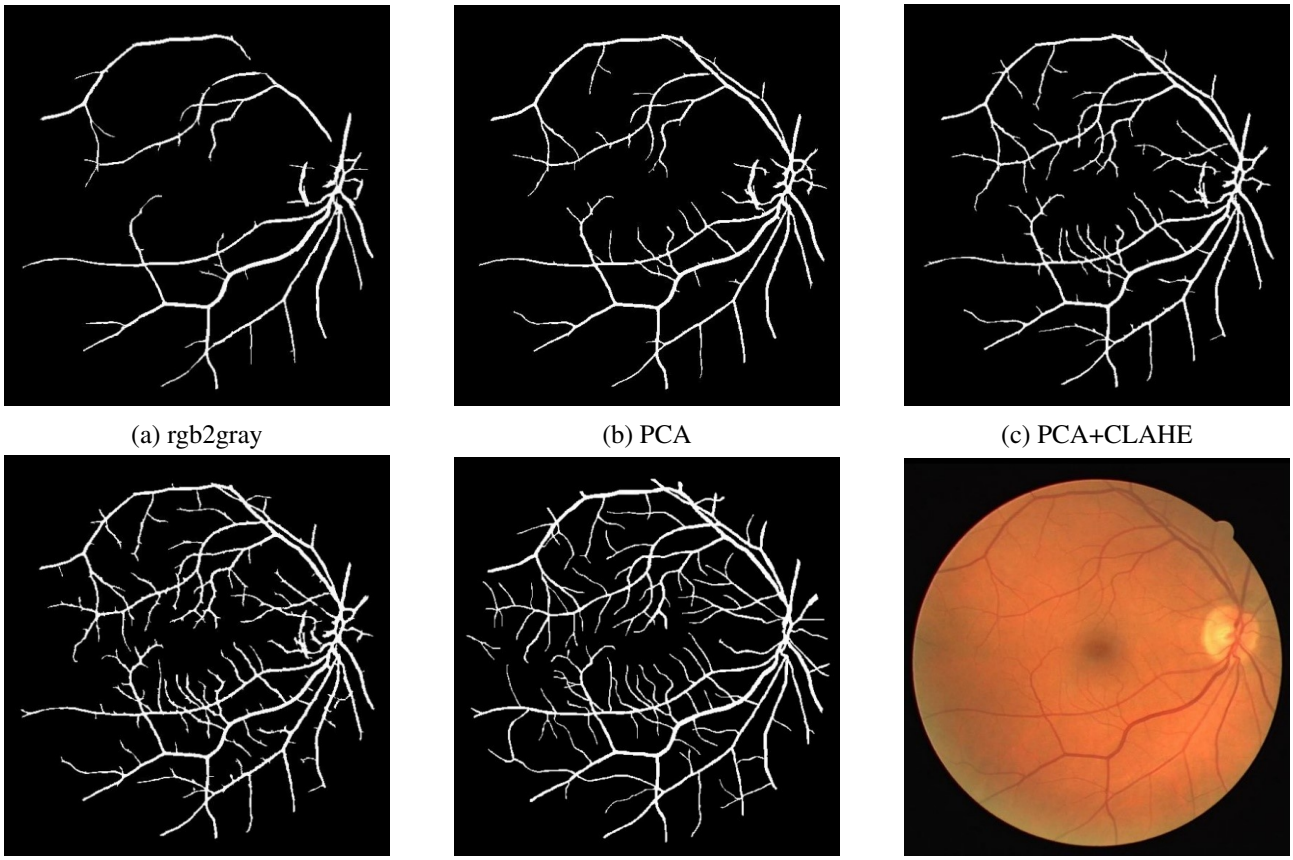

(a) rgb2gray (b) PCA (c) PCA+CLAHE

(d) PCA+MSMO+CLAHE (e) Ground-truth image (f) Original image

Figure 4: Segmented images of 16_test.tif using different pre processing methods for enhancement

from 1 to 15 having interval 1) and n (varying from 1 to 15 having interval 1) for every image of STARE data set. We found average accuracy 95.40 % for α=1, β=1.5, γ=4.5, L=11 and n=4. The method is also practically tested for distinct values of α (varying from 1 to 5 having interval 1), β(varying from 0 to 5.0 having interval 0.5), γ(varying from 0 to 5.0 having interval 0.5), L (varying from 1 to 15 having interval 1) and n (varying from 1 to 15 having interval 1) for every image of HRF data set. We found average accuracy 94.02 % for α=1, β=1.81, γ=1.72, L=11 and n=10.

To build Fréchet match filter kernel, optimal value of α, β, γ and L are chosen. At first, the kernel is assumed to be at origin. We assume a coordinateC_x=[x, y] at the kernel. θ_i is the direction of ith kernel that compares to the vessel at angle θ. Retinal vessels are assumed to scattered in every direction. Hence, it is required to convolve a kernel in each direction. When kernel and vessel are at exact angle, outcome is registered highest. To cover an entire image, 12- kernels with size 15 x 15 are implemented in each direction to detect retinal vessels by revolving kernel at 15 degree corresponding to preceding kernel. These Fréchet kernels having distinct directions are determined by equation (5).

$$Rmi = [cos\theta \quad -sin\theta; \quad sin\theta \quad cos\theta] \tag{5}$$

The corresponding point C_x= [R_x, R_y] in the revolved coordinate system is accomplished by equation (6).

$$P_{x_i} = [Rx, Ry] = P_x * R_{m_i}^T \tag{6}$$

After design of twelve Fréchet match filter kernels, these are convolved with a gray-scale image enhanced by the PCA+MSMO+CLAHE method to generate match-filter response (MFR) image. Figure 5 (c) shows a MFR image produced by the Fréchet match-filter.

3.3 Post-processing

Post processing operation has key role in the accuracy of vessel-segmentation. In the approach, we have applied appropriate and efficient methods for post processing operations. Post processing stage contains the vessels thresholding, length-filtering, masking and complimenting operations. These methods are described as follows:

3.3.1 Thresholding

In the post processing, first a thresholding algorithm is operated on the MFR image to generate binary image. For this, we apply the entropy-based optimal thresholding algorithm on MFR image produced by the Fréchet match-filter. This thresholding method is superior to other existing thresholding methods. The facts behind this are: in this method, possessions between pixel's intensities of MFR image manage the spatial structure in the threshold images and clearly identify vessels from their backgrounds. In this thresholding algorithm, first the gray level co-occurrence matrix (GLCM) is calculated. Thereafter GLCM is grouped in 4 quadrants. I as well as IV quadrants called 'local quadrants' contain gray-level transitions that happens within retinal vessels and backgrounds. Hence, these two quadrants are used to evaluate the local entropy for thresholding. To achieve this, probability of I as well as IV quadrants are determined. Then, entropies are calculated for these two quadrants. Highest value of summation of entropies is chosen as optimal-threshold value. Figure 5 (d) shows the extracted vessels from their background [32][33].

3.3.2 Length Filtering

Vessels extracted by thresholding methods have generally isolated and misclassified pixels. To remove these, we have applied the length filtering technique on extracted vessels. In the literature, we have applied the pixel label propagation and 8-connected neighborhood length filtering methods. The methods are efficient and appropriate in the case of retinal vessels. Figure 5 (e) shows that isolated and misclassified pixels are removed.

3.3.3 Masking

There is a probability that some artifacts may lie on retinal image boundary. To remove these artifacts, we have applied the masking technique. Mask images for STARE and DRIVE are available online. We take masking of input image and perform the logical AND function with corresponding segmented image to eliminate the artifacts. Figure 5 (e) shows that outer artifacts are removed.

3.3.4 Complimenting

In the last of post processing, we perform complement operation on the output image of masking operation. The obtained complemented image is then compared with the corresponding ground truth image for performance evaluation. Figure 5 (f) shows the complemented image.

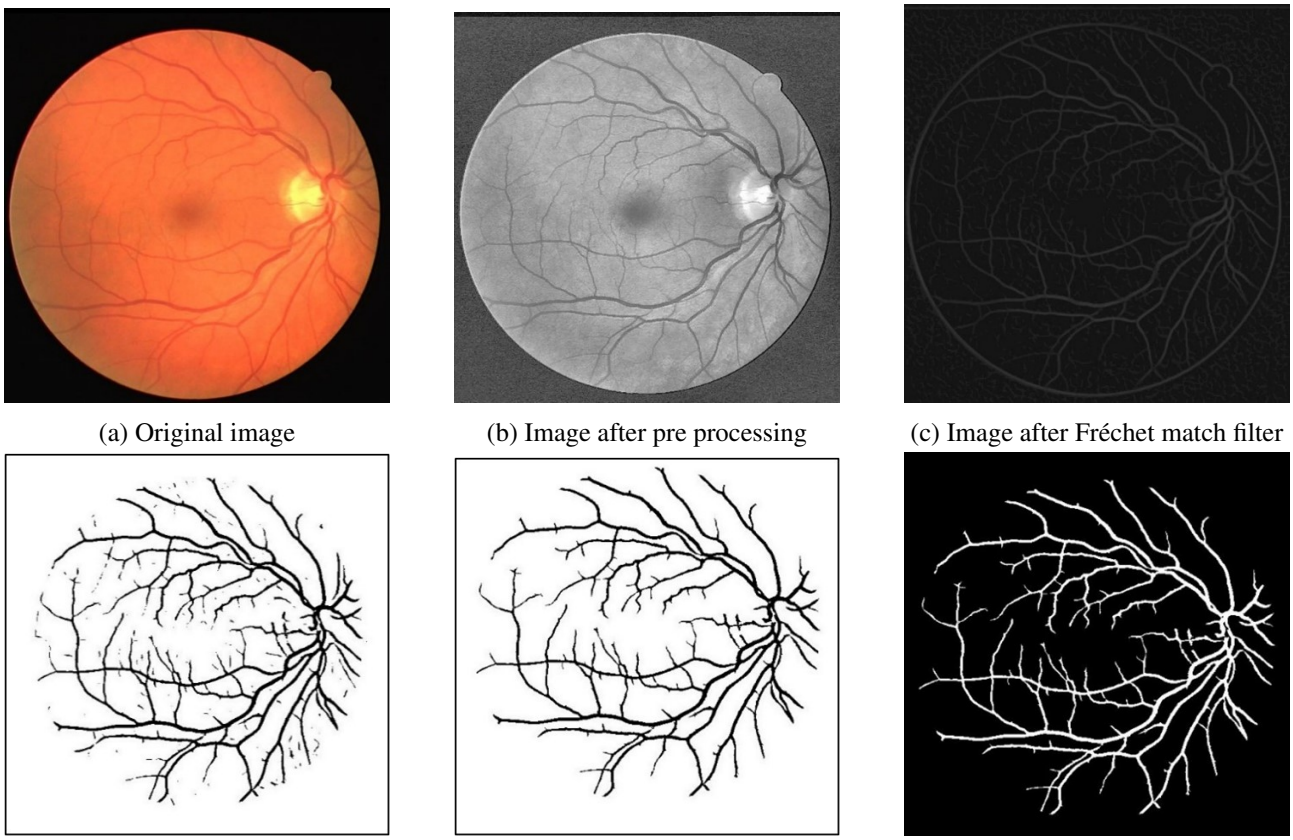

(a) Original image (b) Image after pre processing (c) Image after Fréchet match filter

(d) Image after thresholding (e) Image after length filter,masking (f) Image after complementing

Figure 5: Different images generated at various phases of the proposed method for image 2_test.tif

4 Performance Evaluation

This section contains Experimental Setup, Performance Metrics and Result Analysis subsections.

4.1 Experimental Setup

The method is implemented and validated on various retinal image data sets: HRF, DRIVE and STARE which are standard and freely available online. These data sets briefly described as: DRIVE data set [34] contains 40 images. These images are classified in the training and test sets. Both the sets contain 20 images each. The test set contains two sets of manual segmented images while training contains single set of manually segmented images. Mask images for all 40 images are also available showing region of interest. Each image is captured using Canon CR-5 non mydriatic 3-CCD camera at 45°field of view (FOV). These acquired images contain 8 bits per plane. These images are cropped around FOV. Each image has 565 x 584 dimensions. STARE data set [30] has 400 raw images in which 20 images are selected at random. Out of them, 10 images are healthy and rest images are unhealthy. All the images are acquired by TOPCON-TRV-50 camera with 35° FOV. These images contain 8 bits/plane. Each image has 700 x 605 dimension. Ground truth images are provided by A. Hoover and V. Kouznetsova. HRF data set [4] has 45 original color images out of them 15 images are healthy, 15 images have glaucoma and 15 images have diabetic. HRF data-set has high resolution images. Images are acquired with Canon CR-1 fundus camera at 45° FOV. Every image of this data-set has dimension 3504 x 2336. The method is implemented as well as tested on the MATLAB R2017a on HP desktop having configuration 4-GB RAM, Intel (R), Xeon (R), E3, 3.4 GHz processor and 64 bits windows operating system.

4.2 Performance Metrics

Output of segmentation procedure is basically categorization of the pixels. Each pixel is either non vessel or vessel. Based on this, there may have four possible outputs. These are described as follows:

- True positive (TP): A pixel is identified as a vessel pixel in both segmented and ground truth image.
- True negative (TN): A pixel is identified as a non-vessel pixel in both segmented and ground truth.
- False negative (FN): A pixel is identified as non-vessel pixel in segmented but vessel in ground truth.
- False positive (FP): A pixel is identified as a vessel pixel in segmented and non-vessel in ground truth.

Quantitative performance metrics are calculated on these four outputs. The metrics used in the paper are described as follows:

- Specificity (SP): It is potential of an approach to identify non-vessel pixels. It is defined by equation (7).

$$SP = TN/((TN + FP)) \tag{7}$$

- Sensitivity (SN): It is potential of an approach to identify vessel's pixels. It is described by equation (8).

$$SN = TP/((TP + FN)) \tag{8}$$

- Accuracy (AC): It is ratio of total accurately categorized pixels of an image. It is defined by equation (9).

$$AC = ((TP + TN))/((TP + TN + FN + FP)) \tag{9}$$

- Precision (PR): It is a fraction of the pixels which are true-positive in all pixels identified as vessel pixels.

$$PR = TP/((TP + FP)) \tag{10}$$

- F 1 score: It is a weighted-average of sensitivity and precision. It is described by equation (11).

$$F1score = (2 * TP)/((2 * TP + FP + FN)) \tag{11}$$

4.3 Result Analysis

4.3.1 Quantitative Analysis

In the literature, various quantitative measures like sensitivity, accuracy and specificity are computed. Values of these measures of the proposed method for each image of HRF, DRIVE and STARE data sets are reported in the Tables 7-9 respectively. Values of average specificity, sensitivity and accuracy of the proposed method are compared with various prominent methods of this field for DRIVE and STARE in the Table 10 and 11, respectively. Average accuracy of proposed method is 95.74 % which is found better by 0.30 %, 0.38 %, 0.52 %, 0.61 %, 0.64 %, 1.02 %, 1.05 %, 1.22 %, 3.05 %, 3.74 % and 4.78 % corresponding to currently available approaches viz; Saroj et al., GeethaRamani et al., Singh et al, Singh et al., Memari et al., Lam et al., Zhou et al., Martin et al., Zolfagharnasab et al., Amin et al. and AL-Rawi et al. respectively for DRIVE data set. Like the same way, average accuracy of proposed method is 95.40 % which is found better by 0.31 %, 0.40 %, 0.84 %, 0.91 %, 1.99 %, 2,70 %, 2.73 %, 2.80 %, 4.53 %, 5.64 % and 6.09 % corresponding to currently available approaches viz; Saroj et al., Sreejini et al., Kaba et al., Chen et al., Odstrcilik et al., Singh et al., Hoover et al., Palomera et al., Zhang et al., Kande et al. and Singh et al. respectively for STARE data set. Average accuracy of proposed method is 94.02 % for HRF data set. We have also calculated the precision and F1 score for evaluation of performance. Figure 6 shows the comparison statistics of precision and F1 score. Figure 7 shows the graphical representation of overall performance of the proposed method.

Image	SP	AC	Image	SP	AC	Image	SP	AC
1	0.9944	0.9361	16	0.9872	0.9538	31	0.9918	0.9443
2	0.9934	0.941	17	0.9872	0.9429	32	0.9877	0.9404
3	0.994	0.927	18	0.9859	0.9434	33	0.9984	0.9489
4	0.9883	0.9409	19	0.9848	0.946	34	0.9962	0.9463
5	0.9975	0.9347	20	0.9829	0.949	35	0.9939	0.9464
6	0.9884	0.9408	21	0.9845	0.9358	36	0.993	0.9423
7	0.9981	0.9324	22	0.9845	0.935	37	0.993	0.9532
8	0.9936	0.9375	23	0.9828	0.9321	38	0.9868	0.9481
9	0.9987	0.9432	24	0.9914	0.9405	39	0.9908	0.9483
10	0.9933	0.9433	25	0.9829	0.9298	40	0.9938	0.9518
11	0.9888	0.9385	26	0.988	0.9343	41	0.992	0.9428
12	0.9902	0.9344	27	0.9729	0.9342	42	0.9847	0.9394
13	0.99	0.9352	28	0.9865	0.9413	43	0.9933	0.9464
14	0.9867	0.9339	29	0.975	0.9245	44	0.9903	0.9434
15	0.99	0.9421	30	0.9583	0.9224	45	0.9941	0.9404
					Avg spe.	0.9889	Avg acc.	0.9402

Table 7: Performance of the method for HRF dataset

Image	SP	SN	AC
01_test.tif	0.9722	0.8202	0.9548
02_test.tif	0.9833	0.7645	0.9571
03_test.tif	0.9591	0.7586	0.9553
04_test.tif	0.9929	0.6592	0.9584
05_test.tif	0.9889	0.7139	0.9585
06_test.tif	0.9887	0.6453	0.9555
07_test.tif	0.9784	0.7202	0.951
08_test.tif	0.9797	0.6808	0.9596
09_test.tif	0.9899	0.6653	0.9598
10_test.tif	0.9847	0.6876	0.9563
11_test.tif	0.9795	0.7137	0.9519
12_test.tif	0.9823	0.7237	0.9561
13_test.tif	0.9826	0.6918	0.9599
14_test.tif	0.9696	0.7986	0.9581
15_test.tif	0.9639	0.8112	0.9591
16_test.tif	0.9826	0.7663	0.9589
17_test.tif	0.9893	0.6322	0.9553
18_test.tif	0.9825	0.7658	0.9614
19_test.tif	0.9685	0.8608	0.9557
20_test.tif	0.9847	0.7757	0.9655
Average	0.9802	0.7328	0.9574

Table 8: Performance of the method for DRIVE

Image	SP	SN	AC
im0001.ppm	0.962	0.8374	0.9501
im0002.ppm	0.9802	0.7566	0.9565
im0003.ppm	0.9528	0.7662	0.9334
im0004.ppm	0.9849	0.7254	0.9596
im0005.ppm	0.9825	0.7329	0.9583
im0044.ppm	0.9889	0.6216	0.9524
im0077.ppm	0.9725	0.7191	0.9485
im0081.ppm	0.9794	0.6516	0.9513
im0082.ppm	0.9925	0.6123	0.9609
im0139.ppm	0.9739	0.7485	0.9538
im0162.ppm	0.9766	0.7001	0.9522
im0163.ppm	0.987	0.6778	0.9558
im0235.ppm	0.9736	0.7085	0.9469
im0236.ppm	0.9644	0.7907	0.9495
im0239.ppm	0.9637	0.7961	0.9509
im0240.ppm	0.9846	0.7233	0.9602
im0255.ppm	0.9849	0.6519	0.956
im0291.ppm	0.9763	0.7786	0.9598
im0319.ppm	0.9697	0.832	0.9575
im0324.ppm	0.9834	0.7657	0.9665
Average	0.9766	0.7298	0.954

Table 9: Performance of the method for STARE

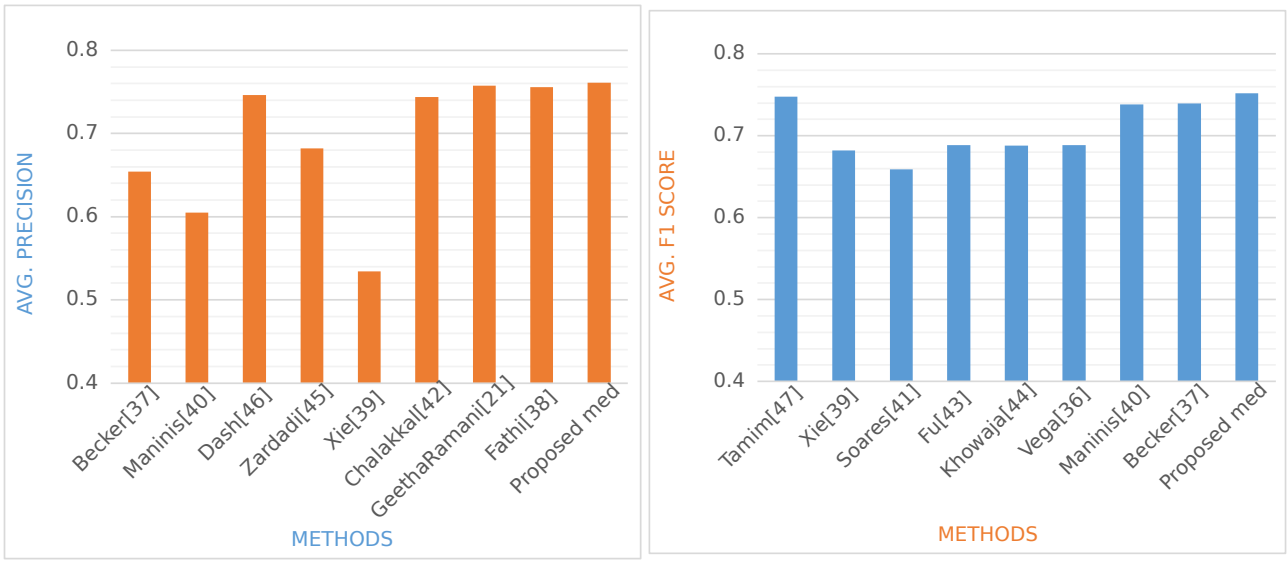

Figure 6: Comparison statistics of precision and F1 score for DRIVE dataset

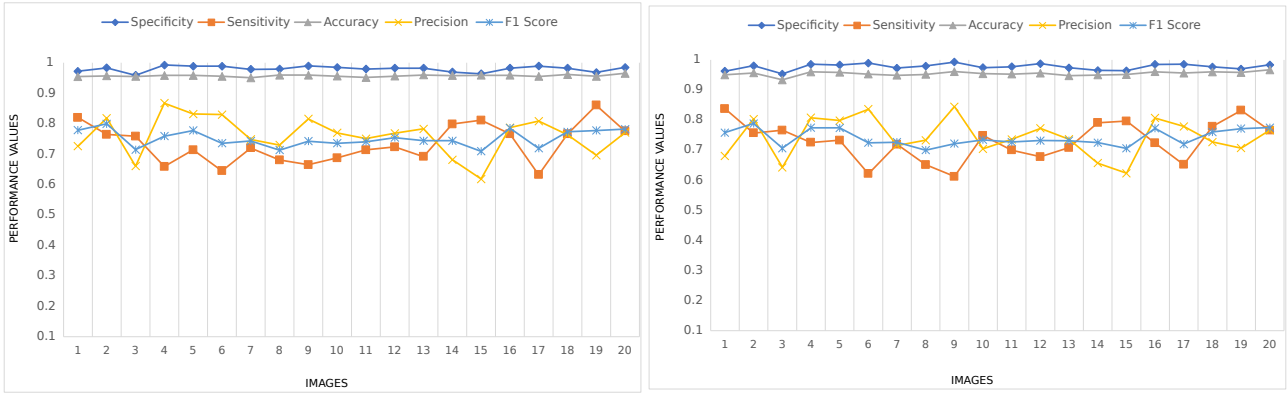

Figure 7: Graphical representation of the performance of the method for DRIVE and STARE, respectively

Author, Year, Ref.	SP	SN	AC
Rawi et al. [28]	0.9553	0.5993	0.9096
Zolfa. et al. [9]	0.9714	0.6239	0.9269
Memari et al. [1]	0.965	0.782	0.951
Zhou et al. [5]	0.9674	0.8078	0.9469
Geetha. et al. [21]	0.9778	0.7079	0.9536
Amin et al. [19]			0.92
Marín et al. [20]	0.9801	0.7067	0.9452
Singh et al. [26]	0.9739	0.7171	0.9513
Lam et al. [15]			0.9472
Singh et al. [7]	0.9708	0.7594	0.9522
Saroj et al. [6]	0.9761	0.7307	0.9544
Proposed approach	0.9802	0.7328	0.9574

Table 10: Comparison of methods for DRIVE

Author, Year, Ref.	SP	SN	AC
Hoover et al. [30]	0.9567	0.6751	0.9267
Kande et al. [27]			0.8976
Zhang et al. [31]	0.9736	0.7373	0.9087
Pal. et al. [35]	0.9449	0.769	0.926
Ods. et al. [4]	0.9512	0.7847	0.9341
Kaba et al. [8]	0.9672	0.7619	0.9456
Sre. et al. [13]	0.9687	0.7172	0.95
Singh et al.[11]	0.9072	0.8389	0.8931
Chen et al. [14]	0.9696	0.7295	0.9449
Singh et al. [7]	0.9376	0.7939	0.927
Saroj et al. [6]	0.9724	0.7278	0.9509
Proposed approach	0.9766	0.7298	0.954

Table 11: Comparison of methods for STARE

4.3.2 Qualitative Analysis

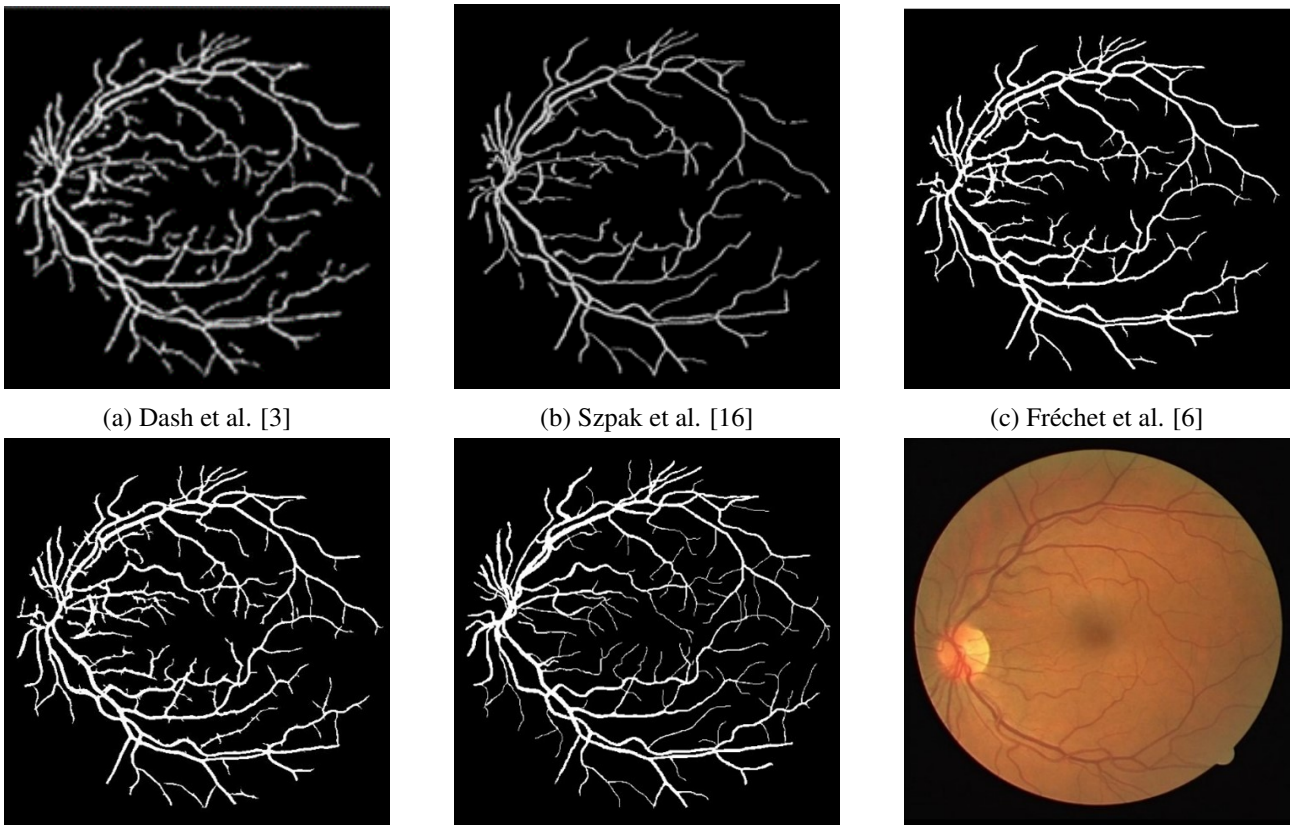

(a) Dash et al. [3] (b) Szpak et al. [16] (c) Fréchet et al. [6]

(d) Proposed segmented-image (e) Ground-truth image (f) Original image

Figure 8: Comparison of segmented images generated by various methods for image 1_test.tif

5 Conclusion

Diabetes, hypertension, obesity, glaucoma etc. have become greater threat to human life today. Information about these diseases can be obtained from retinal blood vessels. Therefore, many researchers have proposed various methods to segment retinal blood vessels. Most researchers have focused only on segmentation process. Pre processing plays vital role in accuracy of vessel segmentation. Hence, the proposed method not only apply efficient segmentation method i.e. the Fréchet match filter but also introduces a novel method called MSMO method for pre processing. We have tested and validated the proposed method on DRIVE, STARE and HRF data sets. The average accuracy of the proposed method is 95.74 %, 95.40 % and 94.02 % for DRIVE, STARE and HRF data sets, respectively. Obtained results demonstrate that the proposed method outperforms over latest and prominent findings of this area. The cause of improved performance is the better pre processing and segmentation methods.

References

[1] N. Memari, A. R. Ramli, M. I. B. Saripan, S. Mashohor, M. Moghbel, ”Retinal blood vessel segmentation by using match filtering and fuzzy c-means clustering with integrated level set method for

diabetic retinopathy assessment", *Journal of Medical and Biological Engineering* 38:713-738, 2019. https://doi.org/10.1007/s40846-018-0454-2

[2] J. Almotri, K. Elleithy, A. Elleithy, "Retinal vessels segmentation techniques and algorithms: a survey", *Applied Sciences, MDPI* 8(155):1-31, 2018. https://doi.org/10.3390/app8020155

[3] J. Dash, N. Bhoi, "Detection of retinal blood vessels from ophthalmoscope images using morphological approach", *Electronic Letter on Computer Vision and Image Analysis* 16:1-14, 2017. https://doi.org/10.5565/rev/elcvia.913

[4] J. Odstrcilik, R. Kolar, A. Budai, J. Hornegger, J. Jan, J. Gazarek, T. Kubena, P. Cernosek, O. Svoboda, E. Angelopoulou, "Retinal vessel segmentation by improved match filtering: evaluation on a new high-resolution fundus image database", *IET Image Processing* 7(4):373–383, 2013. https://doi.org/10.1049/iet-ipr.2012.0455

[5] L. Zhou, Q. Yu, X. Xu, Y. Gu, J. Yang, "Improving dense conditional random field for retinal vessel segmentation by discriminative feature learning and thin-vessel enhancement", *computer Methods and Programs in Biomedicine* 148:13-25, 2017. https://doi.org/10.1016/j.cmpb.2017.06.016

[6] S. K. Saroj, R. Kumar, N. P. Singh, "Fréchet PDF based matched filter approach for retinal blood vessels segmentation", *Computer Methods and Programs in Biomedicine* 194:1-17, 2020. https://doi.org/10.1016/j.cmpb.2020.105490

[7] N. P. Singh, R. Srivastava, "Retinal blood vessels segmentation by using gumbel probability distribution function based match filter", *Computer Methods and Programs in Biomedicine* 129:40-50, 2016. https://doi.org/10.1016/j.cmpb.2016.03.001

[8] D. Kaba, C. Wang, Y. Li, A. Salazar-Gonzalez, X. Liu, A. Serag, "Retinal blood vessels extraction using probabilistic modelling", *Health Information Science Systems* 2(1):1-10, 2014. https://doi: 10.1186/2047-2501-2-2

[9] H. Zolfagharnasab, A. R. Naghsh-Nilchi, "Cauchy based match filter for retinal vessels detection", *Journal of Medical Signals and Sensors* 4(1):1-26, 2014. https://doi: 10.4103/2228-7477.128432

[10] M. M. Fraz, P. Remagnino, A. Hoppe, B. Uyyanonvara, A. R. Rudnicka, C. G. Owen, S. A. Barman, "Blood vessel segmentation methodologies in retinal images–a survey", *Computer Methods and Programs in Biomedicine* 108(1):407–433, 2012. https://doi.org/10.1016/j.cmpb.2012.03.009

[11] N. P. Singh, R. Srivastava, "Extraction of retinal blood vessels by using an extended match filter based on second derivative of gaussian", *Proceedings of the National Academy of Sciences*, India, 89:269–277, 2019. https://doi.org/10.1007/s40010-017-0465-3

[12] J. Seo, S. D. Kim, "Novel pca-based color-to-gray image conversion", *Image Processing (ICIP), International Conference of IEEE*, 2279–2283, 2013. https://doi.org/10.1109/ICIP.2013.6738470

[13] K. S. Sreejini, V. K. Govindan, "Improved multiscale match filter for retina vessel segmentation using PSO algorithm", *Egyptian Informatics Journal* 16(3):253–260, 2015. https://doi.org/10.1016/j.eij.2015.06.004

[14] Y. Chen, "A labeling-free approach to supervising deep neural networks for retinal blood vessel segmentation", *arXiv 2017, arXiv:1704.07502*, 2017. https://doi.org/10.48550/arXiv.1704.07502

[15] B. S. Lam, Y. Gao, A. W. C. Liew, "General retinal vessel segmentation using regularization-based multiconcavity modelling", *Medical Imaging, IEEE Transactions* 29(7):1369–1381, 2010. https://doi.org/10.1109/TMI.2010.2043259

[16] Z. L. Szpak, J. R. Tapamo, "Automatic and interactive retinal vessel segmentation", *South African Computer Journal* 40:23-30, 2008.

[17] N. Salem, A. Shams, H. Malik, "Medical image enhancement based on histogram algorithms", *International Learning and Technology Conference* 163:300-311, 2019. https://doi.org/10.1016/j.procs.2019.12.112

[18] S. S. Negi, B. Gupta, "Survey of various image enhancement techniques in spatial domain using MATLAB", *Proceedings of International Journal of Computer Applications* 8-18, 2014.

[19] M. A. Amin, H. Yan, "High speed detection of retinal blood vessels in fundus image using phase congruency", *Soft Computing* 15(6):1217–1230, 2011. https://doi.org/10.1007/s00500-010-0574-2

[20] D. Marín, A. Aquino, M. E. Gegúndez-Arias, J. M. Bravo, "A new supervised method for blood vessel segmentation in retinal images by using gray-level and moment invariants-based features", *Medical Imaging, IEEE Transactions* 30(1):146–158, 2011. https://doi.org/10.1109/TMI.2010.2064333

[21] R. GeethaRamani, L. Balasubramanian, "Retinal blood vessel segmentation employing image processing and data mining techniques for computerized retinal image analysis", *Bioinformatics and Biomedical Engineering* 5:1-16, 2015. https://doi.org/10.1016/j.bbe.2015.06.004

[22] K. Zuiderveld, "Contrast limited adaptive histogram equalization", *Graphics Gems; Academic Press Professional, Inc.*, San Diego, USA, 474–485, ISBN 0-12-336155-9, 1994.

[23] N. Solouma, A.-B. M. Youssef, Y. Badr, Y. M. Kadah, "Real-time retinal tracking for laser treatment planning and administration", *Medical Imaging, International Society for Optics and Photonics* 1311–1321, 2001. https://doi.org/10.1117/12.431010

[24] Y. Wang, S. C. Lee, "A fast method for automated detection of blood vessels in retinal images", *Signals, Systems and amp; Computers, Conference Record of the Thirty-First Asilomar Conference* 2:1700–1704, 1997. https://doi.org/10.1109/ACSSC.1997.679192

[25] A. Pinz, S. Bernögger, P. Datlinger, A. Kruger, "Mapping the human retina", *Medical Imaging, IEEE Transactions* 17(4):606–619, 1998. https://doi.org/10.1109/42.730405

[26] N. P. Singh, R. Srivastava, "Weibull probability distribution function-based match filter approach for retinal blood vessels segmentation", *Advances in Computational Intelligence, Advances in Intelligent Systems and Computing* 509:427-437, 2017. https://doi.org/10.1007/978-981-10-2525-9_4

[27] G. B. Kande, P. V. Subbaiah, T. S. Savithri, "Unsupervised fuzzy based vessel segmentation in pathological digital fundus images", *Journal of medical systems* 34(5):849–858, 2010. https://doi.org/10.1007/s10916-009-9299-0

[28] M. Al-Rawi, M. Qutaishat, M. Arrar, "An improved match filter for blood vessel detection of digital retinal images", *Computers in Biology and Medicine* 37(2):262–267, 2007.

[29] G. Tascini, G. Passerini, P. Puliti, P. Zingaretti, "Retina vascular network recognition", *proceedings of Medical Imaging*, 1993.

[30] A. Hoover, V. Kouznetsova, M. Goldbaum, "Locating blood vessels in retinal images by piecewise threshold probing of a match filter response", *Medical Imaging, IEEE Transactions* 19(3):203–210, 2000. https://doi.org/10.1109/42.845178

[31] Y. Zhang, W. Hsu, M. L. Lee, "Detection of retinal blood vessels based on nonlinear projections", *Journal of Signal Processing Systems* 5(1):103–112, 2009. https://doi.org/10.1007/s11265-008-0179-5

[32] N. R. Pal, S. K. Pal, "Entropic thresholding", *Signal processing* 16(2):97–108, 1989. https://doi.org/10.1016/0165-1684(89)90090-X

[33] T. Chanwimaluang, G. Fan, "An efficient blood vessel detection algorithm for retinal images using local entropy thresholding", *Circuits and Systems, Proceedings, International Symposium* 5:21–23, 2003. https://doi.org/10.1109/ISCAS.2003.1206162

[34] J. Staal, M.D. Abramoff, M. Niemeijer, M.A. Viergever, B. van Ginneken, "Ridge- based vessel segmentation in color images of the retina", *IEEE Transaction on Medical Imaging* 23(4):501–509, 2004. https://doi.org/10.1109/TMI.2004.825627

[35] M. A. Palomera-Pérez, M. E. Martinez-Perez, H. Benítez-Pérez, J. L. Ortega-Arjona, "Parallel multiscale feature extraction and region growing application in retinal blood vessel detection", *IEEE Transactions on Information Technology in Biomedicine* 14(2):500–506, 2010. https://doi.org/10.1109/TITB.2009.2036604

[36] R. Vega, G. Sanchez-Ante, L.E. Falcon-Morales, H. Sossa, E. Guevara, "Retinal vessel extraction using lattice neural networks with dendritic processing",*Computers in Biology and Medicine* 58:20–30, 2015.

[37] C. Becker, R. Rigamonti, V. Lepetit, P. Fua, "Supervised feature learning for curvilinear structure segmentation", *Proceeding of MICCAI* 8149:526-533, 2013.

[38] A. Fathi, A R. Naghsh-Nilchi, "Automatic wavelet-based retinal blood vessels segmentation and vessel diameter estimation", *Biomedical Signal Processing and Control* 8(1):71–80, 2013.

[39] S. Xie, Z. Tu, "Holistically-nested edge detection", *Proceedings of ICCV* 1395-1403, 2015.

[40] K. K. Maninis, J. Pont-Tuset, P. Arbeláez, L. V. Gool, "Deep retinal image understanding", *Proceedings of MICCAI* 140-148, 2016.

[41] J. V. B. Soares, J. J. G. Leandro, R. M. Cesar, H. F. Jelinek, M. J. Cree, "Retinal vessel segmentation using the 2-D gabor wavelet and supervised classification", *IEEE Transanction on Medical Imaging* 25(9):1214-1222, 2006.

[42] R. J. Chalakkal, W. H. Abdulla, "Improved vessel segmentation using curvelet transform and line operators", *proceedings of APSIPA Annual Summit and Conference* pp. 2041-2046, 2018.

[43] H. Fu, Y. Xu, D. W. K. Wong, J. Liu, "Retinal vessel segmentation via deep learning network and fully connected conditional random fields", *Proceedings of the IEEE 13th International Symposium on Biomedical Imaging*, Prague, Czech Republic, 698–701, 2016.

[44] S. A. Khowaja, P. Khuwaja, I. A. Ismaili, "A framework for retinal vessel segmentation from fundus images using hybrid feature set and hierarchical classification", *Signal Image Video Process* 13:379–387, 2019. https://doi.org/10.1007/s11760-018-1366-x

[45] M. Zardadi, N. Mehrshad, S. M. Razavi, "Unsupervised segmentation of retinal blood vessels using the Human visual system line detection model", *Journal of Information Systems and Telecommunication* 4(2):125-133, 2016. https://doi.org/10.7508/jist.2016.02.008

[46] J. Dash, N. Bhoi, "A thresholding-based technique to extract retinal blood vessels from fundus images", *Future Computing and Informatics Journal* 1-7, 2017. https://doi.org/10.1016/j.fcij.2017.10.001

[47] N. Tamim, M. Elshrkawey, G. A. Azim, H. Nassar, "Retinal Blood Vessel Segmentation Using Hybrid Features and Multi-Layer Perceptron Neural Networks", *Symmetry, MDPI* 1-27, 2020. https://doi.org/10.3390/sym12060894